Generalized Iterative Dichotomy PAPR Reduction Method for Multicarrier Waveforms

Khaled Tahkoubit, Hmaied Shaiek, Daniel Roviras, Salim Faci, Adda Ali-Pacha

IEEE Access
Multidisciplinary | Rapid Review | Open Access Journal

Received July 4, 2021, accepted August 2, 2021, date of publication August 5, 2021, date of current version August 23, 2021.

Digital Object Identifier 10.1109/ACCESS.2021.3102848

Generalized Iterative Dichotomy PAPR Reduction Method for Multicarrier Waveforms

KHALED TAHKOUBIT[1,2], (Student Member, IEEE), HMAIED SHAIEK[2], (Member, IEEE), DANIEL ROVIRAS[2], (Senior Member, IEEE), SALIM FACI[3], (Senior Member, IEEE), AND ADDA ALI-PACHA[1]

[1]LaCoSi, USTO-MB, Oran 31000, Algeria
[2]CEDRIC/LAETITIA, Conservatoire National des Arts et Métiers (CNAM), 75003 Paris, France
[3]Électronique, Systèmes de Communication et Microsystèmes (ESYCOM), Univ Gustave Eiffel, CNRS, Conservatoire National des Arts et Métiers (CNAM), ESIEE Paris, 75141 Paris, France

Corresponding author: Khaled Tahkoubit (khaled.tahkoubit@univ-usto.dz)

ABSTRACT 5th generation systems (5G) will be based on Orthogonal Frequency Division Multiplexing (OFDM) multicarrier modulation technique. This modulation has a very high Peak to Average Power Ratio (PAPR). This high PAPR is a drawback when nonlinear Power Amplifiers (PA) are operated near the saturation region, for energy efficiency purposes, due to in-band and out-of-band impairments. In this paper, a new PAPR reduction technique called Iterative Dichotomy PAPR (IDP) is proposed. This method is suited for any multicarrier modulation and is studied here using realistic PA model. For evaluating the signal distortions, two main metrics have been considered to evaluate the performance of IDP technique: bit error rate (BER) and power spectrum density (PSD). The analytical expressions of the IDP technique for any dichotomy order M is firstly described and subsequently the energy efficiency for different M values is compared. We have shown that the proposed IDP method reduces the PAPR by $2.2dB$ for $M = 2$ and $4dB$ for $M = 4$. Regarding the energy efficiency, for the same Error Vector Magnitude (EVM) and the same PA power consumption, the output signal power obtained with the IDP based technique outperforms classical OFDM by 20%, 50% and 80% for $M = 2$, $M = 3$ and $M = 4$, respectively.

INDEX TERMS Bit error rate, error vector magnitude, iterative dichotomy PAPR, OFDM, PA, PAPR, PSD.

I. INTRODUCTION

Upcoming 5th generation systems wireless communication systems are expected to support a wide range of services with diverse requirements. One of the main concerns for 5G systems is the improvement of energy efficiency. Furthermore, Multiple-Input Multiple-Output (MIMO) and massive MIMO technologies will be generalized in 5G. Multiplying power amplifiers in MIMO transmitting chains, together with the constraint of an increased energy efficiency and low cost are antagonist constraints. With MIMO transmitters, low cost PA are needed but could have eventually quite poor properties concerning the linearity. On the other hand, for increasing energy efficiency, it is well known that PA must be operated near to their saturation region [1]. When combining these two parameters, the transmitted signal will experience in-band and out-of-band distortions. Severe degradations are generated on the signal at the output of the amplifier by these non-linearities, such as spectral regrowth and increased Error Vector Magnitude (EVM) [2]. These impairments will be furthermore emphasized if a high Peak to Average Power Ratio (PAPR) waveforms are used.

Designing a linear wideband PA for 5G at mm-Wave frequency is very challenging, different wideband mm-wave PA designs were presented in [3] and [4]. Most radio frequency (RF) cellular PAs are designed in semiconductors due to superior frequency response and breakdown performance. Power amplifiers based gallium nitride (GaN) technology are one of the technology candidates for 5G PA. The GaN technology support the PA performance, efficiency, and power by facilitating the transmission of multiple data streams with greater capacity and thermal efficiency. The authors in [5] proposed a 2.6GHz class-AB PA based on GaN technology. This PA achieves nearly 200MHz bandwidth while maintaining optimal performance with extremely great Power Added Efficiency (PAE) reaching 70%. We have based our power efficiency comparison on this PA technology.

The associate editor coordinating the review of this manuscript and approving it for publication was Chen Chen.

In 5G systems, multicarrier modulations have been planed because of their resilience towards frequency selective channels. Recently, OFDM [6] has win the standardization battle. This waveform has been also adopted in many other standards like LTE-A [7], Wi-Fi [8], and so on. As any multicarrier modulation, the OFDM signal has a variable envelope, which can be quantified by the PAPR. The amplification of such a waveform suffers from the nonlinear behavior of the PA, especially when it is working near to the saturation region.

To avoid the nonlinear distortions induced by the PA, it is necessary to escape the saturation region to operate continuously in the linear region. However, this solution leads to a very low energy efficiency and is incompatible with user equipments powered with batteries. An alternative solution concerns the PAPR reduction of the emitted waveform before PA and thit is the scope of this paper.

In the literature, several PAPR reduction techniques have been proposed for OFDM systems. The interested reader can refer to surveys as [9], [10] for example. Some techniques for reducing PAPR are downward compatible such as clipping [11], signal adding [12] and tone reservation techniques [13]. Downward compatibility means that the receiver does not need any side information from the transmitter. Other PAPR reduction techniques do not respect the downward compatibility principle, such as, selective mapping [14], Partial Transmit Sequence [15] and coding technique [16]. Downward compatibility techniques are highly preferred in order to have a receiver independent of the used PAPR reduction technique. Recently, we proposed new PAPR reduction technique with downward compatibility [17]. This method has been applied to OFDM signal but it could be used for any kind of multicarrier modulation. The main idea of the proposed method is to decompose the multicarrier signal into M signals with much lower PAPR, by using an algorithm called Iterative Dichotomy PAPR (IDP). The M signals are amplified by M power amplifiers, combined with a suitable combiner and then fed to a single antenna. This configuration can suffer from electrical delays between the PA outputs but with a same PA in integrated technology, the combined signals are well controlled and consequently the unpairing between the PAs is low [18]. In addition, the phase shift between the signals to be summed is very low. When $M = 2$, the IDP technique has an architecture similar to a linear amplification using nonlinear components (LINC) technique [19]. In the LINC method, the wireless signal is converted into two signals with null PAPR. These two signals are amplified by two efficient amplifiers in each branch and recombined to form an amplified wireless signal. Nevertheless, in LINC, the two generated signals before the amplification process have very high power, unlike the IDP method where the power of the two signals to be amplified are much lower. We have compared in [20] the energy efficiency between these two methods and we have shown that the performances with IDP technique are better. In [17], we have proposed the IDP method and we have restricted our theoretical analysis to the order $M = 2$.

Regarding our previous work, the main contributions of this paper are:

- Generalization of the theoretical analysis of the PAPR reduction achieved by the IDP technique, for any dichotomy order M. A recurrent method is proposed in order to compute the PAPR for any dichotomy order M. Simulation and theoretical results are compared.
- The analysis of the energy efficiency of the proposed IDP approach compared to classical OFDM based scheme. The analysis considered three parameters: Error Vector Magnitude (EVM), output radiated power and Direct Current (DC) consumed power.
- Study of the computational complexity of the IDP technique and compare it to other downward compatibility PAPR reduction techniques such as TR and Clipping.

The remainder of this paper is organized as follows. Section II provides a background on OFDM, PAPR characterization, power amplifier models, adjacent channel power ratio (ACPR) and EVM. In section III, an illustration of IDP method is given, as well as, the theoritical analysis of the PAPR calculation for any value of dichotomy order M. The general method/algorithm for building the transmitter architecture, along with the energy efficiency computation of the IDP method are presented in section IV. In section V, numerical results are shown as well as computational complexity analysis. Finally, the conclusion of this paper is given in section VI.

II. BACKGROUND

A. SYSTEM MODEL

In this paper we are concerned by the 5G downlink cells where classical CP-OFDM is used. OFDM is an orthogonal multicarrier system based on the Inverse Fast Fourier Transform (IFFT) and a rectangular shaping filter. The time domain signal can be written:

$$x(n) = \frac{1}{\sqrt{N}} \sum_{k=0}^{N-1} X(k) e^{\frac{j2\pi kn}{N}}, \quad n = 0, 1, \ldots, N-1 \quad (1)$$

where $X(k) = [X(0), X(1), \ldots, X(N-1)]$ is a vector of complex QAM symbols, k is the subcarrier index and N is the total number of subcarriers.

The PAPR parameter is defined as the ratio between the maximum peak power to the average power of the signal over a defined time interval T (generally, T is taken equal to the length of the OFDM symbol, N samples).

$$PAPR = 10log_{10}\left(\frac{\underset{0\le n\le N-1}{max}\left\{|x(n)|^2\right\}}{\mathbb{E}\left\{|x(n)|^2\right\}}\right) \quad (2)$$

where $\mathbb{E}\{.\}$ is the statistical expectation operator.

The PAPR is a random variable representing the signal dynamic. Commonly, PAPR is represented by the Complementary Cumulative Distribution Function (CCDF) [21]. The CCDF is the probability that the PAPR is greater than a fixed

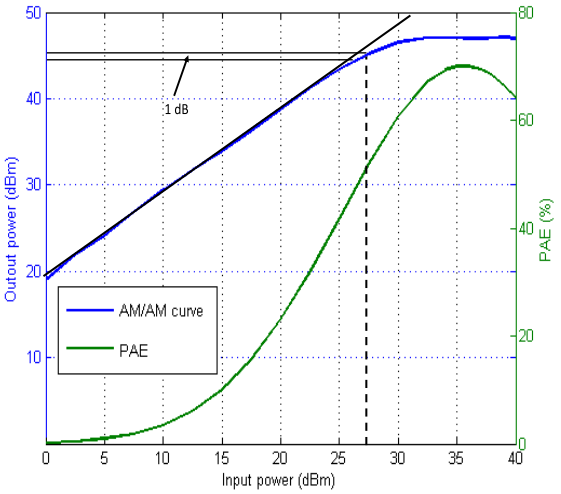

FIGURE 1. Output power, PAE vs. input power of the used PA [3].

PAPR, called $PAPR_0$.

$$CCDF_{PAPR}(PAPR_0) = Pr\,(PAPR > PAPR_0) \tag{3}$$

B. PA MODELS AND DC POWER

In this study, we use a realistic PA model. The considered PA is a 2.6GHz class-AB based on GaN transistor with a power gain of $19dB$, a maximum output power of $56W$ and a power added efficiency (PAE) of 70%. The AM/AM and PAE characteristics are shown in Fig.1

It is well known that, the consumed power P_{DC} for high input power is equal to:

$$P_{DC} = \frac{P_{out} - P_{in}}{PAE} \tag{4}$$

where P_{out} is the emitted signal power and P_{in} is the input signal power.

It is often necessary to take a given backoff from the power compression point at $1dB$ in order to operate the amplifier in the linear region. Then, we use the input backoff (IBO) to analyse the system performances. Let $P_{out,1dB}$ be the output power at 1dB compression point and $P_{in,1dB}$ the corresponding input power. The IBO is the ratio between the input power at the 1dB compression point and the average input power of the signal.

$$IBO[dB] = 10log_{10}\frac{P_{out,1dB}}{P_{in}}, [dB] \tag{5}$$

According to Fig. 1, the $P_{in,1dB}$ for the used model is equal to $27.5dB$.

C. ADJACENT CHANNEL POWER RATIO

The nonlinear amplification of a multicarrier signal occupying a given spectral bandwidth (useful channel) generates a spreading of its spectrum which results in an increased power spectral density in the adjacent channels. This phenomenon is known as spectral regrowth or out-of-band radiation.

The spectral regrowth induced by the PA is characterized by the Adjacent Channel Power Ratio (ACPR). ACPR is defined as the ratio of adjacent channel power P_{AC} to the main channel power P_{MC}. We call "ACPR" higher ("up"), calculated by considering the upper adjacent channel power ($P_{AC_{(up)}}$), and "ACPR" lower ("low"), calculated by considering the lower adjacent channel power ($P_{AC_{(low)}}$).

$$ACPR_{(up,low)}[dB] = 10log_{10}\left(\frac{P_{AC_{(up,low)}}}{P_{MC}}\right) \tag{6}$$

D. ERROR VECTOR MAGNITUDE

To measure the in-band impact of nonlinearities on the useful signal, we use the Error Vector Magnitude (EVM) which is the ratio between the root mean square average amplitude of the error vector to ideal signal amplitude reference. The error vector is a vector between the ideal constellation point and the received point. In our case, the EVM is a parameter that evaluates the constellation distortion due to fluctuations in gain and phase of the amplified signal. The EVM computation requires demodulation of the OFDM signal to recover the I and Q signals. The EVM can be written as:

$$EVM = \sqrt{\frac{\mathbb{E}\left\{\left|X(k) - \hat{X}(k)\right|^2\right\}}{\mathbb{E}\left\{|X(k)|^2\right\}}} \tag{7}$$

where, $X(k)$ and $\hat{X}(k)$ is respectively the complex QAM transmitted symbol and received symbol over subcarrier k.

III. IDP REDUCTION METHOD

A. METHOD DESCRIPTION

The Iterative Dichotomy PAPR method [17] is a downward compatibility method, i.e. there is no side information sent to the receiver. The signal $x(n)$ is decomposed into M signals, $x_m(n)$, $(m = 1, \ldots, M)$, using IDP algorithm. The M parameter is called the dichotomy order of the IDP method. The summation of all sub-signals gives the original signal: $x(n)$. We can write the signal at the output of the IDP processing as follows:

$$x(n) = \sum_{m=1}^{M} x_m(n) \tag{8}$$

The sub-signals $x_m(n)$, $m = 1, \ldots, M$, are then amplified in each branches by a suitable amplifier. However, the sub-signals are scaled by an adequate scalar gain α_m to ensure the targeted IBO_m of the signal at the input of the m^{th} sub-amplifier.

As signals $x_m(n)$, have a very low correlation, we can write

$$P_x = \sum_{m=1}^{M} P_{x_m} \tag{9}$$

where, P_x is the power of the original signal $x(n)$ and P_{x_m} is the power of the sub-signal $x_m(n)$.

The amplified M sub-signals are recombined by a suitable circuit and the constructed signal is transmitted by the

antenna. We assume a perfect synchronized recombination of the M sub-signals at the output of the amplifiers. In addition, if perfect linear amplification is used, the signal $y(n)$ should be equal to an amplified version of $x(n)$.

B. THEORETICAL ANALYSIS OF THE PAPR ACHIEVED BY IDP METHOD

In [17], we have restricted our theoretical analysis to a dichotomy order $M = 2$. In the following, we will establish theoretical analysis for PAPR reached by IDP method for any higher dichotomy order. The general idea of IDP method is to decompose the original signal $x(n)$ as follows:

$$x(n) = \sum_{m=1}^{M} z_m(n) + \varepsilon_M(n) \tag{10}$$

where $z_m(n)$ is a signal with constant envelope and $\varepsilon_M(n)$ is an error signal.

A constant envelope signal is a signal whose PAPR is equal to $0dB$, meaning that it is insensitive to nonlinear amplification. On the contrary, the error signal $\varepsilon_M(n)$ is a signal that has a high PAPR value. This error signal can be subdivided and added to the M sub-signals $z_m(n)$ as follows:

$$x_m(n) = z_m(n) + \frac{R_m}{\sum_{p=1}^{M} R_p}\varepsilon_M(n) \tag{11}$$

The sub-signals $x_m(n)$ are then the sum of a constant envelope signal $z_m(n)$ with an additional high PAPR signal. In order to control the PAPR of the M sub-signals, only a certain part of $\varepsilon_M(n)$ is added to $z_m(n)$. This part is related to the mean absolute value of $z_m(n)$. By doing so, we ensure that the variable part of the error signal $\varepsilon_M(n)$, to be added to the signal $z_m(n)$, is proportional to its power. The IDP algorithm steps are given in Algorithm 1.

Algorithm 1 IDP Algorithm

1: Initialization: $\varepsilon_0(n) = x(n)$, $m = 0$
2: $R_{m+1} = E\{|\varepsilon_m(n)|\}$
3: $z_{m+1}(n) = R_{m+1}.e^{j\varphi_m(n)}$, $\varphi_m(n)$: the phase of $\varepsilon_m(n)$
4: $\varepsilon_{m+1}(n) = \varepsilon_m(n) - z_{m+1}(n)$
5: **if** $m < M$ **then**
6: $\quad m = m + 1$, go to 2
7: **else**
8: $\quad$ Compute $x_m(n)$, $m = 1, \ldots, M$ following equation (11)
9: **end if**

At each iteration of the IDP algorithm we have to compute R_m. For $m = 1$, R_1 is the expectation of $|x(n)|$. It is well-known that if the number of subcarriers N is very large, the OFDM signal $x(n)$ can be considered as a centered complex Gaussian signal with uncorrelated real and imaginary parts with a variance equal to σ_x^2. R_1 is then given by:

$$R_1 = E\{|x(n)|\} = \int_0^{+\infty} u\frac{u}{\sigma_x^2}e^{-\frac{u^2}{2\sigma_x^2}}du \tag{12}$$

According to the law of the unconscious statistician (LOTUS) [22], we can write:

$$\begin{aligned} R_2 &= E\{||x(n)| - R_1|\} = \int_0^{+\infty} |u - R_1|\,\frac{u}{\sigma_x^2}e^{-\frac{u^2}{2\sigma_x^2}}du \\ &= \int_0^{R_1} (R_1 - u)\,\frac{u}{\sigma_x^2}e^{-\frac{u^2}{2\sigma_x^2}}du \\ &\quad + \int_{R_1}^{+\infty} (u - R_1)\,\frac{u}{\sigma_x^2}e^{-\frac{u^2}{2\sigma_x^2}}du \end{aligned} \tag{13}$$

Similarly, we have:

$$\begin{aligned} R_3 &= \int_0^{+\infty} ||u - R_1| - R_2|\,\frac{u}{\sigma_x^2}e^{-\frac{u^2}{2\sigma_x^2}}du \\ &= \int_0^{R_1-R_2} [(R_1 - R_2) - u]\,\frac{u}{\sigma_x^2}e^{-\frac{u^2}{2\sigma_x^2}}du \\ &\quad + \int_{R_1-R_2}^{R_1} [u - (R_1 - R_2)]\,\frac{u}{\sigma_x^2}e^{-\frac{u^2}{2\sigma_x^2}}du \\ &\quad + \int_{R_1}^{R_1+R_2} [(R_1 + R_2) - u]\,\frac{u}{\sigma_x^2}e^{-\frac{u^2}{2\sigma_x^2}}du \\ &\quad + \int_{R_1+R_2}^{+\infty} [u - (R_1 + R_2)]\,\frac{u}{\sigma_x^2}e^{-\frac{u^2}{2\sigma_x^2}}du \end{aligned} \tag{14}$$

From equation (11), the synthesis of each partial signal $x_m(n)$ to be amplified by the m^{th} amplifier requires the computation of all the R_m values. That is what we propose in this paper a generalized approach allowing the computation of R_m at any IDP dichotomy order M. To address this point, we define a function $\gamma(B_i, B_j)$ as follows:

$$\gamma(B_i, B_j) = \int_{B_i}^{B_j} \frac{u\,(u - B_i)}{\sigma_x^2}e^{-\frac{u^2}{2\sigma_x^2}}du \tag{15}$$

From equation (13), we can express R_2 as:

$$R_2 = \gamma(R_1, 0) + \gamma(R_1, +\infty) \tag{16}$$

Similarly, from equation (14), we can express R_3 as:

$$\begin{aligned} R_3 = \gamma(R_1 - R_2, 0) + \gamma(R_1 - R_2, R_1) \\ + \gamma(R_1 + R_2, R_1) + \gamma(R_1 + R_2, +\infty) \end{aligned} \tag{17}$$

More generally, we can write at any dichotomy order M:

$$R_M = \sum_{k=1}^{(T_M-1)/2} (\gamma(B_{2k}, B_{2k-1}) + \gamma(B_{2k}, B_{2k+1})) \tag{18}$$

where $T_M = 2^{M-1} + 1$ is the total number of boundaries in the interval $[0, +\infty]$ and B_k are the values of the boundaries.

For example, for R_3 we have the following partition: $[0, (R_1 - R_2), R_1, (R_1 + R_2), +\infty]$. The total number of boundaries $T_3 = 2^{3-1} + 1 = 5$, with $[B_1, B_2, B_3, B_4, B_5] = [0, (R_1 - R_2), R_1, (R_1 + R_2), +\infty)]$.

The boundaries of any dichotomy order M can be computed based on the diagram given in Appendix A and Fig. 10. Additionally, the computation of function $\gamma(B_i, B_j)$ is detailed

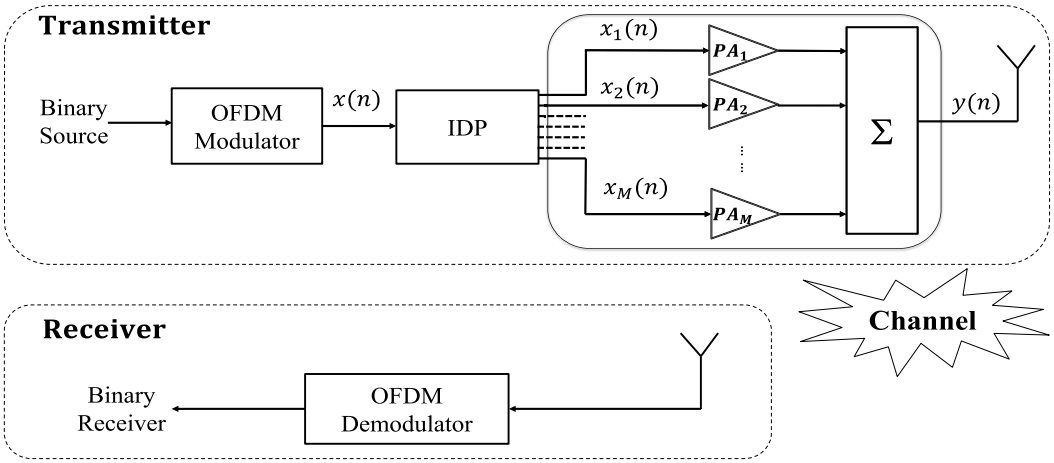

FIGURE 2. Block diagram of an OFDM transceiver using IDP method.

in Appendix B. Finally, using results of Appendix A and B, equation (18) can be rewritten as:

$$R_M = \sum_{k=1}^{(T_M-1)/2} (2B_{2k} - B_{2k-1} - B_{2k+1})\, e^{-\frac{B_{2k}^2}{2\sigma_x^2}} + \sigma_x\sqrt{\frac{\pi}{2}} \times \left[2erfc\left(\frac{B_{2k}}{\sigma_x\sqrt{2}}\right) - erfc\left(\frac{B_{2k-1}}{\sigma_x\sqrt{2}}\right) - erfc\left(\frac{B_{2k+1}}{\sigma_x\sqrt{2}}\right)\right] \tag{19}$$

Let's focus now on the relationship between the PAPR of the original signal $x(n)$ and the one of the final signals $x_m(n)$. We want first to underline that the signals considered for computing the PAPR are $x_m(n)$, given by equation (11).

Considering N samples of the signal $x_m(n)$, the maximum value of $|x_m(n)|$ is given by:

$$\max_{0\le n\le N-1}(|x_m(n)|) = R_m + \frac{R_m}{\sum_{p=1}^{M} R_p} \max_{0\le n\le N-1}(|\varepsilon_M(n)|) \tag{20}$$

with

$$\max_{0\le n\le N-1}(|\varepsilon_M(n)|) = \max_{0\le n\le N-1}(|x(n)|) - \sum_{p=1}^{M} R_p \tag{21}$$

By replacing equation (21) in equation (20), we can write:

$$\max_{0\le n\le N-1}(|x_m(n)|) = R_m + \frac{R_m}{\sum_{p=1}^{M} R_p}\left[\max_{0\le n\le N-1}(|x(n)|) - \sum_{p=1}^{M} R_p\right] \tag{22}$$

After straight forward simplification, we can rewrite equation (22) as:

$$\max_{0\le n\le N-1}(|x_m(n)|) = \frac{R_m}{\sum_{p=1}^{M} R_p} \max_{0\le n\le N-1}(|x(n)|) \tag{23}$$

The PAPR of the signal $x_m(n)$ is given by:

$$PAPR_{x_m} = \frac{\left[\frac{R_m}{\sum_{p=1}^{M} R_p}\right]^2}{P_{x_m}} \max_{0\le n\le N-1}\left(|x(n)|^2\right) \tag{24}$$

Finally, using equations (23), (24), we have:

$$PAPR_{x_m} = \frac{P_x}{P_{x_m}}\left[\frac{R_m}{\sum_{p=1}^{M} R_p}\right]^2 PAPR_x \tag{25}$$

For $M = 2$, we have shown in [17] that the two final signals have quite similar PAPR equal, approximately to 0.6 times the linear PAPR of the original signal.

IV. ENERGY EFFICIENCY

In this section, we study the energy efficiency of the IDP method, by comparing an IDP based OFDM transmitter to a classical one. Fig. 3 shows the transmitters corresponding to the classical OFDM scheme (Fig 3(a)) and the IDP based (Fig 3(b)). We remind that with the IDP method, the original signal $x(n)$ is decomposed into M signals using equation (11).

For the amplification process we use a single power amplifier PA_0 to amplify the OFDM signal $i(n)$., while we use power amplifiers $PA_1, PA_2, \ldots, PA_M$ to amplify signals $i_1(n)$, $i_2(n)$, $\ldots$, $i_M(n)$, in the IDP based transmitter, as depicted by 3(b). The PA_0 model is based on the $2.6GHz$ GaN amplifier charateristics with $19dB$ power gain and a PAE up to 70%. The other amplifier models are derived from the PA_0 model by adjusting the power compression points.

In [17], we demonstrated that the signals at the IDP output with $M = 2$, were uncorrelated, with respective average powers equal to:

$$\frac{P_{x_1}}{P_x} = 0.8642 \tag{26}$$

and

$$\frac{P_{x_2}}{P_x} = 0.1358 \tag{27}$$

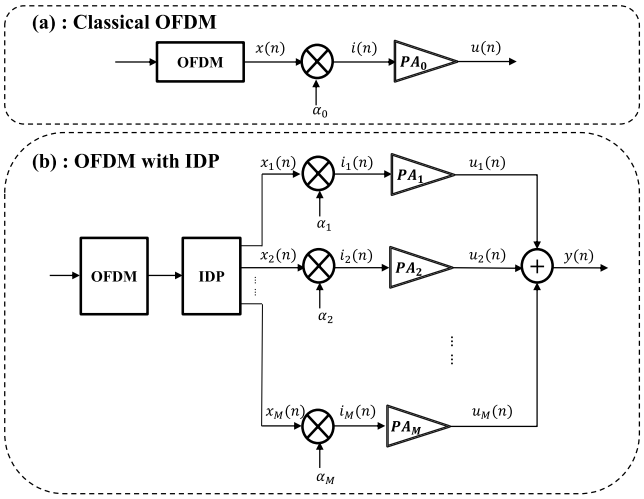

FIGURE 3. OFDM transmitter in presence of PA: (a)-Classical case,(b)-IDP based OFDM.

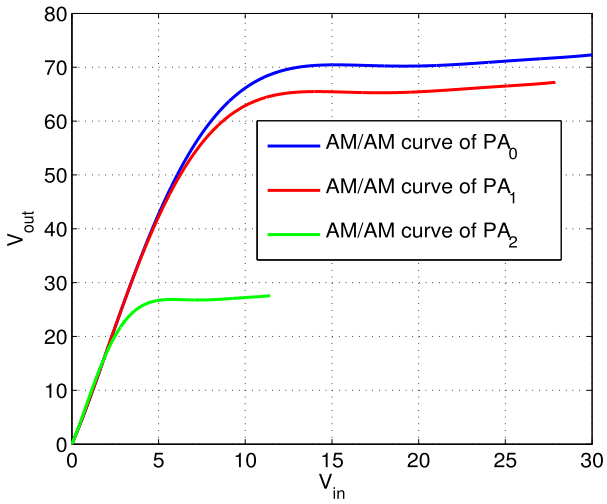

FIGURE 4. PA AM/AM curves PA_0, PA_1 and PA_2.

The linear AM/AM curve of PA_0 plotted in Fig. 1. For a dichotomy order equal to M, PA_1 to PA_M have the same power gain and the same PAE. Nevertheless, because input signals $i_m(t)$ have different powers the AM/AM curve of the m^{th} PA is scaled by factor equal to $\sqrt{P_{x_m}/Px}$ for both input voltage V_{in} and output voltage V_{out}. Fig. 4 gives an example of AM/AM curves for PA_0, PA_1 and PA_2.

In the following, we give more insights on the approaches used to set the parameters of the two schemes in order to compare the energy efficiency. The multiplicative coefficicents $\alpha_0, \alpha_1, \ldots, \alpha_M$ are used to fix the IBO of each PA. From (4), the DC power by the OFDM based scheme is written as:

$$P_{DC_{OFDM}} = \frac{P_u - P_i}{PAE} \tag{28}$$

For the IDP based scheme, the corresponding consumed DC power is equal to:

$$P_{DC_{IDP}} = \sum_{m=1}^{M} \frac{P_{u_m} - P_{i_m}}{PAE} \tag{29}$$

In order to compare the energy efficiency of the two schemes given by Fig. 3, we fixed both consumed DC power and the EVM at the same values and we compare the output signal powers P_y and P_u. To do that, we follow two steps:

Step 1: in order to get the same EVM for signals $u(n)$ and $y(n)$ we fix a common IBO_0 for all power amplifiers PA_0, PA_1 to PA_M. Because the PAPR of $x_m(n)$ signals is lower than the one of the OFDM signal $x(n)$, the expected EVM with IDP method is lower than the EVM of a classical OFDM. Then, we gradually reduce the IBO_m of the differents PA_m used in the IDP based scheme until reaching the same EVM.

Step 2: when both schemes of Fig.3(a) and 3(b) have the same EVM, we enforce a same consumed power P_{DC} for the two schemes and we compare the two output powers.

V. SIMULATION RESULTS

In this section, the simulation results of the IDP algorithm are presented. First, we validate the analytical expression of the PAPR given by (25). Second, we analyse the influence of the dichotomy order M on ACPR and BER. Then, the energy efficiency is studied following the previously described scenario. Finally, the computational complexity of IDP is computed. The simulation results are obtained by generating 10^5 OFDM symbols using $N = 256$ subcarriers and an over-sampling factor $L = 4$. The data symbols have been modulated using a $16 - QAM$ constellation on each subcarrier and the channel model used is the AWGN one.

A. ACCURACY OF ANALYTICAL EQUATIONS

1) PAPR PERFORMANCES

the PAPR CCDF of the IDP method with M equal to 2, 3 and 4 and the original OFDM signal are shown in Fig. 5. At $CCDF = 10^{-3}$, the PAPR of the OFDM is about $10.8dB$. At this PAPR CCDF, there is a gain of $2.2dB$, in terms of PAPR, at a dichotomy order $M = 2$. For a higher dichotomy order M, we can reach a gain of $3.4dB$ and $4dB$ with $M = 3$ and $M = 4$, respectively. We can also notice a good agreement between numerical results and theoretical expectations which approves the accuracy of equation (25).

B. IMPACT OF THE DICHOTOMY ORDER M

1) PSD AND ACPR

as we pointed out in Section II, the nonlinear amplification causes out-of-band radiation over adjacent channel. However, the use of PAPR reduction techniques minimize this spectral re-growth. Thus, we evaluate the impact of the IDP technique on the power spectral density after amplification.

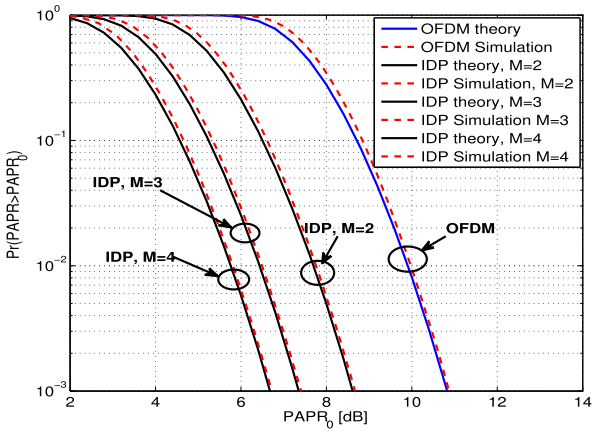

FIGURE 5. CCDF of the PAPR for OFDM and IDP schemes. Modulation format 16 − *QAM*, $N = 256$ and $L = 4$.

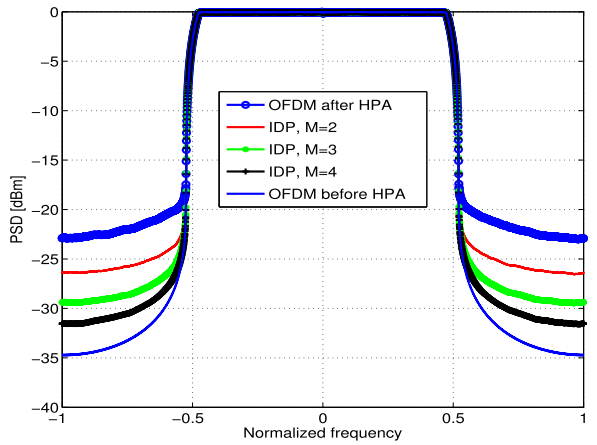

FIGURE 6. PSD before and after PA ($IBO = 3dB$), for OFDM system and IDP based system for $M = 2, 3, 4$.

TABLE 1. ACPR for OFDM system and IDP system for $M = 2, 3, 4$.

ACPR [dB]	IBO=3dB	IBO=6dB	IBO=9dB
OFDM	-27.46	-29.90	-30.87
IDP, M=2	-27.02	-30.95	-31.16
IDP, M=3	-29.25	-31.60	-31.71
IDP, M=4	-30.85	-31.92	-31.98

In Fig. 6, we show the normalized PSD of the input OFDM signal and the output OFDM signal in the classical and IPD configurations with $IBO = 3dB$. We can notice the imporvement achieved by the IDP method for three dichotomy values: $M = 2, 3, 4$. The PSD simulation results confirm the spectral re-growth induced by the use of PA. Additionally, it can be clearly seen from Fig. 6, that performance, in terms of spectral de-growth, increases with the IDP dichotomy order M.

The ACPR performances are summarized in table 1 and show better ACPR value for a tageted IBO with a higher dichotomy order. It should be noticed that the improvement achieved by the IDP method is better for low IBO values. This is what it is looked for in the IDP configuration because using a high IBO value means that amplifiers operate in the linear region inducing low energy efficiency.

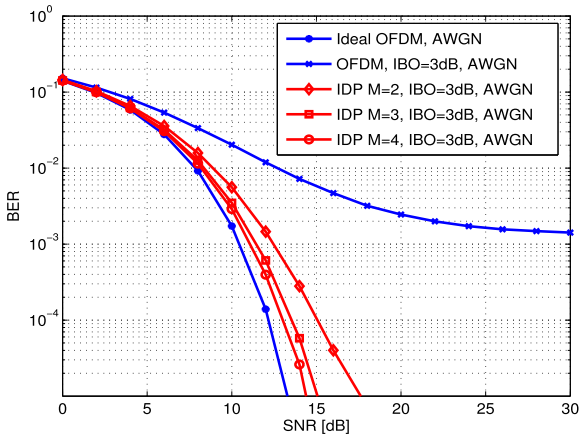

FIGURE 7. BER performances of the classical OFDM and IDP method over AWGN channel.

TABLE 2. Ratio between emitted power for the same DC consumption power and EVM.

IBO for OFDM PA [dB]	3	4	5	6	7	8	9	10
M=2	1.25	1.26	1.27	1.28	1.29	1.30	1.34	1.47
M=3	1.52	1.53	1.54	1.54	1.54	1.54	1.58	1.69
M=4	1.78	1.78	1.79	1.80	1.81	1.82	1.89	2

2) BIT ERROR RATE (BER)

in Fig. 7 we plot the BER of the OFDM signal without nonlinear distortion (curve labelled "ideal OFDM, AWGN") together with the BER when all the PA (PA_0, PA_1, PA_2 and PA_3) are operated at an IBO equal to $3dB$. Without PAPR reduction, we can notice from the curve labelled "OFDM, $IBO = 3dB$, AWGN" a strong degradation of the BER due to the high PAPR of the signal at the input of PA_0. With PAPR reduction using IDP method, we can see from curves labelled "IDP $M = 2$, $IBO = 3dB$, AWGN", "IDP $M = 3$, $IBO = 3dB$, AWGN" and "IDP $M = 4$, $IBO = 3dB$, AWGN" a small degradation of the BER compared to the linear case, thanks to the PAPR reduction achieved by the IDP algorithm. We can also conclude that this PAPR reduction, achieved by the IDP algorithm, reduces the power of the in-band nonlinear distortion noise, decreasing, thus, the BER floor.

C. ENERGY EFFICIENCY

Here we present simulation results giving the comparison between the energy efficiency of the two schemes of Fig.3 described in section IV. For this comparaison, we fixed both EVM and consumed DC power ($P_{DC_{OFDM}} = P_{DC_{IDP}}$) to determine the output power of each configuration.

Table 2 shows the ratio between power delivered by the IDP system P_y and the output power of the OFDM system P_u. We can observe from these results that the output power is

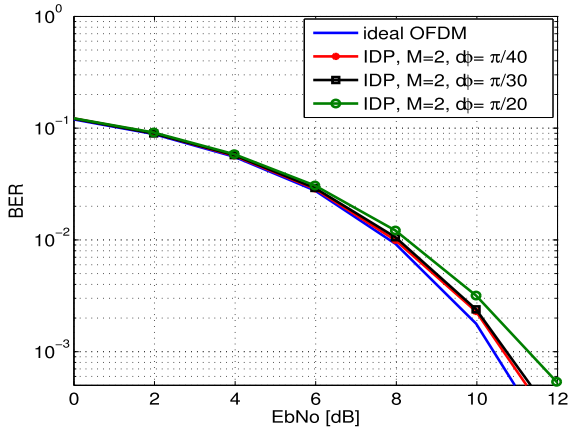

FIGURE 8. Inluence of phase offset of IDP recombined signal on BER.

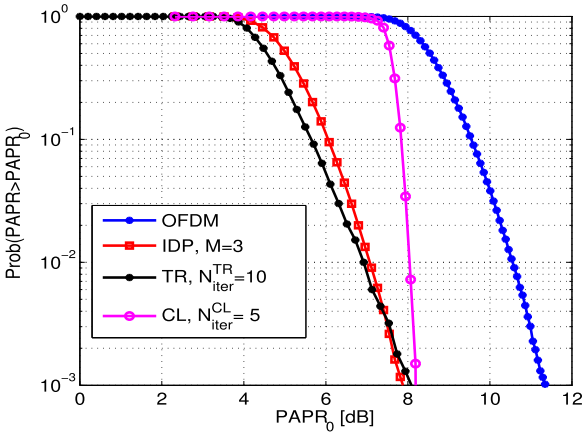

FIGURE 9. PAPR performance with IDP, CL and TR schemes.

higher with IDP system. With $M = 2$, the output power P_y is 1.26 times the power P_u, that give an improvement of 26% for $IBO = 3dB$. Furthermore, the higher is the dichotomy order M, the higher is the ratio between output powers. For $M = 3$ and $M = 4$ there is an improvement of 53% and 78% for $IBO = 3dB$. We restricted our simulations to $IBO = 10dB$, because the PAE is less than 20% at this value.

D. PA SYNCHRONIZATION

In this section, we performed BER simulation by considering the synchronization errors in the summation of the M amplified signals. In [23], authors have shown that phase imbalance between the two branches is limited to 2.2° when the two PA are integrated on the same substrate over a 10GHz bandwidth.

Fig. 8 illustrates the BER performance of the OFDM signal with IDP method when phase missalignement ($d\phi$) is applied between signals $x_1(n)$ and $x_2(n)$ (see Fig. 2). We use $d\phi = \pi/40$, $d\phi = \pi/30$, and $d\phi = \pi/20$ ie 4.5°, 6°, and 9°, respectively. When $d\phi = \pi/40$ and $\pi/30$, we can see, for a $BER = 10^{-3}$ that the resulting performances are verry close to the one obtained when no phase offset is experienced between the two amplifiers. While, when $d\phi = \pi/20$, there is a small degradation of $1dB$ at $BER = 10^{-3}$.

E. COMPLEXITY

As the proposed PAPR reduction method is downward compatible, no modification/side information is required at the receiver side. For complexity analysis, we compare the proposed IDP method to two other PAPR reduction and downward compatible methods, which are classical clipping and filtering (CL) method [11] and tone reservation (TR) method [13]. In this section, the complexity will be assessed based on the total number of complex multiplications required by the three methods: CL, TR and IDP.

Let's N being the total number of subcarriers, M the IDP dichotomy order and L the over-sampling factor. CL and TR are two iterative approaches and require respectively N_{iter}^{CL} and N_{iter}^{TR} iterations. For these techniques, each iteration requires $NLlog_2(NL)$ complex multiplications. Regarding the proposed IDP scheme, and based on equation (11), this method requires NLM complex multiplications. In order to compare the complexity of the three methods (CL, TR and IDP) we have selected operating conditions that give the same PAPR performance.

TABLE 3. PAPR reductions of the IDP, CL and TR schemes with different numbers of iterations.

	Complex multiplication Number (Generic value)	Complex multiplication Number
IDP	NLM	3072
CL	$N_{iter}^{CL} NL \log_2(NL)$	51200
TR	$N_{iter}^{TR} NL \log_2(NL)$	102400

Fig. 9 illustrates the PAPR performance of the IDP, TR and CL schemes. To assess the PAPR reduction complexity of the IDP scheme, we have compared it to CL and TR schemes at a similar PAPR of around $8dB$ for a CCDF probability of 10^{-3}. To reach this PAPR, the IDP scheme requires the dichotomy order $M = 3$. However, CL and TR require respectively $N_{iter}^{CL} = 5$ and $N_{iter}^{TR} = 10$ iterations. The number of tones reserved by the TR method is equal to 13.

Table 3 presents the number of required complex multiplications for the three techniques, to reach a PAPR of $8dB$ for a CCDF probability of 10^{-3}. From these results, it can be clearly seen that the IDP is the method requiring lowest complexity. From the numerical operating conditions fixed here, the number of complex multiplications required by CL and TR is respectively 16.5 and 33 times higher than that of IDP.

VI. CONCLUSION

In this paper, we have proposed a generalized iterative dichotomy technique for reducing the PAPR of multicarrier modulated signals. This technique, named IDP, is based on splitting any multicarrier modulated signal into M signals with reduced PAPR. The gain, in terms of PAPR reduction, increases with the dichotomy order M. The first part of this paper focused on PAPR theoretical analysis for an OFDM system. Regarding PAPR reduction performance, our theoretical analysis are in total agreement with simulation results

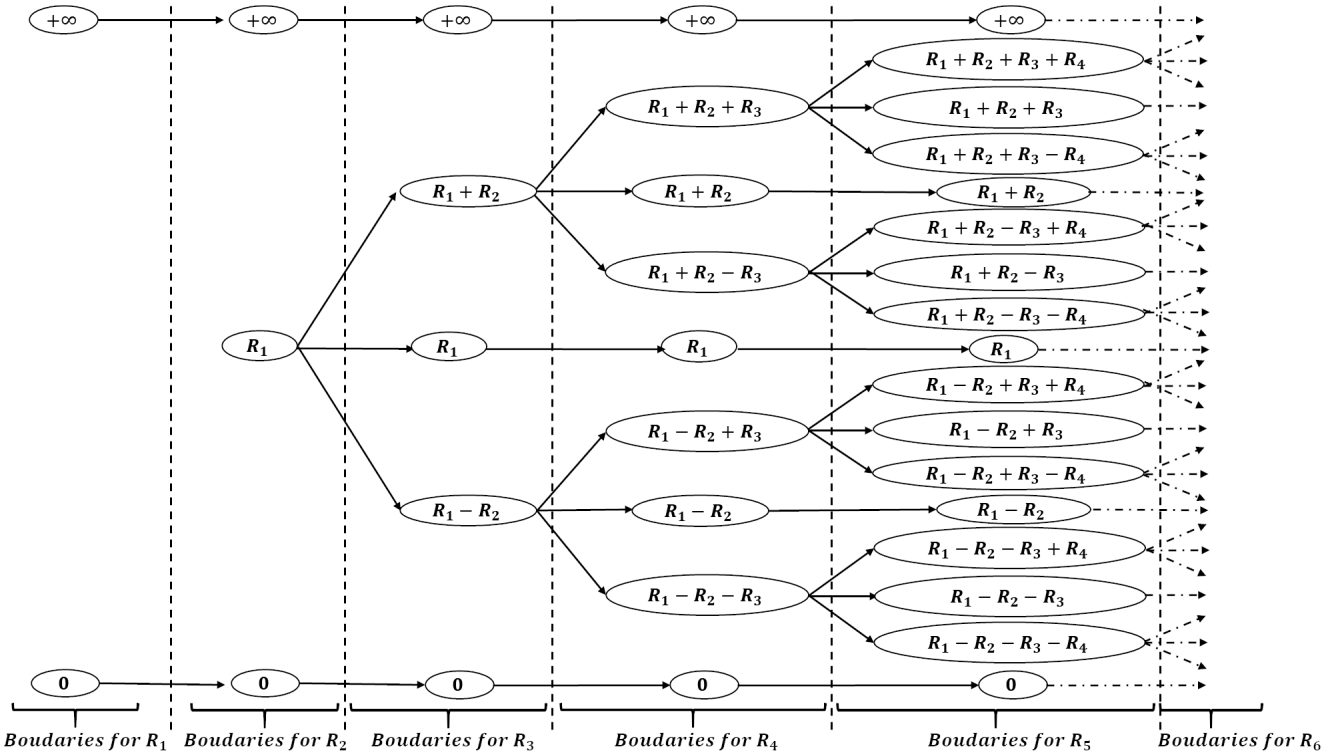

FIGURE 10. **Boundaries computation for any dichotomy order *M*.**

at any dichotomy order M. The PAPR analysis has been completed by studying the impact of the proposed algorithm on PSD and BER.

The second part of the analysis has been dedicated to the performance study of the IDP technique from an energy efficiency point of view. To do so, we have compared an IDP based transmitter to a classical one in presence of realistic class-AB power amplifiers. The three parameters considered to compare the two schemes are the output power, the DC consumed power and the EVM. We have chosen to compare the two shcemes in terms of transmitted power for equal EVM and DC consumed power. We have demonstrated that the IDP based system outperforms the classical OFDM one, while requiring low implementation complexity, compared to other downward compatibility PAPR reduction techniques, such as tone reservation and clipping and filtering. Finally, we would like to underline that all the analysis carried out in this paper are related to OFDM signals. However, they could be easily applied to any other multicarrier waveforms.

APPENDIX A
BOUNDARIES COMPUTATION

For a given dichotomy order M, the equation (18), allows the computation of R_M parameter as following:

$$R_M = \sum_{k=1}^{(T_M-1)/2} \{\gamma(B_{2k}, B_{2k-1}) + \gamma(B_{2k}, B_{2k+1})\} \quad (30)$$

where $T_M = 2^{M-1} + 1$ is the total number of boundaries in the interval $[0, +\infty]$ and B_k are the values of the boundaries.

The diagram of Fig. 10 shows how are computed the boundaries B_k, for any dichotomy order M.

Let B_i, $i = 1, \ldots, T_M$ be the boundaries required to compute R_M. In these boundaries B_1 is the first one, B_2 is the second and so on. For any dichotomy order M, the first boundary B_1 is always equal to 0 and the last one: B_{T_M} is equal to $+\infty$. In order to find the boundaries $B_2, B_3, \ldots, B_{T_M-1}$, we use the diagram given by Fig. 10.

At a dichotomy order M, an even index boundary $B_2 i$ give birth to three boundaries over the dichotomy order $M + 1$. These boundaries are equal to $B_2 i - R_M$, $B_2 i$, $B_2 i + R_M$ (see Fig. 10).

As an example, lets compute the boundaries at the dichotomy order $M = 4$ from those related to dichotomy order $M = 3$. As demonstrated in subsection III-B, the boundaries at $M = 3$ are: $B_1^{M=3} = 0$, $B_2^{M=3} = R_1 - R_2$, $B_3^{M=3} = R_1$, $B_4^{M=3} = R_1 + R_2$ and $B_5^{M=3} = +\infty$. By using the diagram of Fig. 10, we can compute the boundaries at the dichotomy order $M = 4$, the boundaries are:

- $B_1^{M=4} = B_1^{M=3} = 0$,
- $B_2^{M=4} = B_2^{M=3} - R_3 = R_1 - R_2 - R_3$,
- $B_3^{M=4} = B_2^{M=3} = R_1 - R_2$,
- $B_4^{M=4} = B_2^{M=3} + R_3 = R_1 - R_2 + R_3$,
- $B_5^{M=4} = B_3^{M=3} = R_1$,
- $B_6^{M=4} = B_4^{M=3} - R_3 = R_1 + R_2 - R_3$,
- $B_7^{M=4} = B_4^{M=3} = R_1 + R_2$,
- $B_8^{M=4} = B_4^{M=3} + R_3 = R_1 + R_2 + R_3$,
- $B_9^{M=4} = B_9^{M=3} = +\infty$.

APPENDIX B
$\gamma(B_i, B_j)$ COMPUTATION

Any dichotomy order M, fixed by the IDP algorithm, requires the computation of all R_m, $m = 1 \ldots M$. In equation (11), we have demonstrated that the computation of any R_m is based on the generic function $\gamma(i, j)$ written as:

$$\gamma(i,j) = \int_i^j \frac{u\,(u-i)}{\sigma^2} e^{-\frac{u^2}{2\sigma^2}} du \tag{31}$$

The computation of $\gamma(i, j)$ can be done through partial integration, by writing:

$$\begin{aligned}\gamma(i,j) &= \int_i^j \frac{u^2}{\sigma^2} e^{-\frac{u^2}{2\sigma^2}} du - \frac{i}{\sigma^2}\int_i^j u e^{-\frac{u^2}{2\sigma^2}} du \\ &= I + V\end{aligned} \tag{32}$$

where:

$$\begin{aligned}I = \int_i^j \frac{u^2}{\sigma^2} e^{-\frac{u^2}{2\sigma^2}} du &= i e^{-\frac{i^2}{2\sigma^2}} - j e^{-\frac{j^2}{2\sigma^2}} \\ &+\sigma\sqrt{\frac{\pi}{2}}\left[erfc\frac{i}{\sigma\sqrt{2}} - erfc\frac{j}{\sigma\sqrt{2}}\right]\end{aligned} \tag{33}$$

and

$$V = -\frac{i}{\sigma^2}\int_i^j u e^{-\frac{u^2}{2\sigma^2}} du = i\left[e^{-\frac{j^2}{2\sigma^2}} - e^{-\frac{i^2}{2\sigma^2}}\right] \tag{34}$$

where: $erfc(r) = \frac{2}{\sqrt{\pi}}\int_r^{+\infty} e^{-v^2} dv$

Equation (34) can be simplified as follows:

$$\begin{aligned}\gamma(i,j) &= (i-j)\, e^{-\frac{j^2}{2\sigma^2}} \\ &+\sigma\sqrt{\frac{\pi}{2}}\left[erfc\left(\frac{i}{\sigma\sqrt{2}}\right) - erfc\left(\frac{j}{\sigma\sqrt{2}}\right)\right]\end{aligned} \tag{35}$$

From equation (18) and based on the explanation given in Appendix A, we can write:

$$R_M = \sum_{k=1}^{(T_M-1)/2} \left(\gamma(B_{2k}, B_{2k-1}) + \gamma(B_{2k}, B_{2k+1})\right) \tag{36}$$

where $T_M = 2^{M-1}+1$ is the total number of boundaries in the interval $[0, +\infty]$ and B_k are the values of these boundaries, with $B_1 = 0$ and $B_{T_M} = +\infty$.

Equation (36) can be rewritten as:

$$\begin{aligned}R_M = &\sum_{k=1}^{(T_M-1)/2} (B_{2k} - B_{2k-1})\, e^{-\frac{B_{2k-1}^2}{2\sigma^2}} \\ &+ (B_{2k} - B_{2k+1})\, e^{-\frac{B_{2k+1}^2}{2\sigma^2}} \\ &+\sigma\sqrt{\frac{\pi}{2}}\left[2erfc\left(\frac{B_{2k}}{\sigma\sqrt{2}}\right) - erfc\left(\frac{B_{2k-1}}{\sigma\sqrt{2}}\right)\right. \\ &\left.-erfc\left(\frac{B_{2k+1}}{\sigma\sqrt{2}}\right)\right]\end{aligned} \tag{37}$$

Finally, a recurrence relation, for computing R_{M+1}, from R_M is given by:

$$\begin{aligned}R_{M+1} = &\sum_{k=1}^{(T_M-1)/2} \left(\gamma(B_{2k} - R_M, B_{2k-1}) + \gamma(B_{2k} - R_M, B_{2k})\right. \\ &\left.+\gamma(B_{2k} + R_M, B_{2k}) + \gamma(B_{2k} + R_M, B_{2k+1})\right)\end{aligned} \tag{38}$$

REFERENCES

[1] E. Costa, M. Midrio, and S. Pupolin, "Impact of amplifier nonlinearities on OFDM transmission system performance," *IEEE Commun. Lett.*, vol. 3, no. 2, pp. 37–39, Feb. 1999.
[2] R. Schmogrow, "Error vector magnitude as a performance measure for advanced modulation formats," *IEEE Photon. Technol. Lett.*, vol. 24, no. 1, pp. 61–63, Jan. 1, 2012.
[3] Y.-W. Chang, T.-C. Tsai, J.-Y. Zhong, J.-H. Tsai, and T.-W. Huang, "A 28 GHz linear and efficient power amplifier supporting wideband OFDM for 5G in 28 nm CMOS," in *IEEE MTT-S Int. Microw. Symp. Dig.*, Los Angeles, CA, USA, Aug. 2020, pp. 1093–1096.
[4] H. He, T. Ge, Y. Kang, L. Guo, and J. S. Chang, "A 40 MHz bandwidth, 91% peak efficiency, 2.5 W output power supply modulator with dual-mode sigma–delta control and adaptive biasing amplifier for multistandard communications," *IEEE Trans. Power Electron.*, vol. 35, no. 9, pp. 9430–9442, Sep. 2020.
[5] Z. Chen, K. Li, K. Jin, C. Huang, P. Li, and L. Geng, "A 2.6 GHz class-AB GaN power amplifier with maximum output power of 56W achieving 70% power added efficiency," in *Proc. 1st Workshop Wide Bandgap Power Devices Appl. Asia (WiPDA Asia)*, May 2018, pp. 328–331.
[6] R. V. Nee and R. Prasad, *OFDM for Wireless Multimedia Communications*. Norwood, MA, USA: Artech House, 2000.
[7] J. Lee, Y. Kim, Y. Kwak, J. Zhang, A. Papasakellariou, T. Novlan, and C. Sun, "LTE-advanced in 3GPP rel-13/14: An evolution toward 5G," *IEEE Commun. Mag.*, vol. 54, no. 3, pp. 36–42, Mar. 2016.
[8] M. J. Cook and I. Ong, "Comcast cable communications LLC," U.S. Patent 10 321 268, Feb. 15, 2019.
[9] T. Jiang and Y. Wu, "An overview: Peak-to-average power ratio reduction techniques for OFDM signals," *IEEE Trans. Broadcast.*, vol. 54, no. 2, pp. 257–268, Jun. 2008.
[10] U. B. Mahadevaswamy and M. N. Geetha, "A comparative survey on PAPR reduction in OFDM signal," in *Proc. Int. Conf. Electr., Electron., Commun., Comput. Optim. Techn. (ICEECCOT)*, Mysuru, Karnataka, Dec. 2016, pp. 123–126.
[11] J. Armstrong, "Peak-to-average power reduction for OFDM by repeated clipping and frequency domain filtering," *Elect. Lett.*, vol. 38, no. 8, pp. 246–247, Aug. 2002.
[12] D. Guel and J. Palicot, "Artificial signals addition for reducing PAPR of OFDM systems," in *Proc. IEEE Int. Symp. Signal Process. Inf. Technol.*, Sarajevo, Bosnia Herzegovina, Dec. 2008, pp. 281–286.
[13] K. Tani, Y. Medjahdi, H. Shaiek, R. Zayani, and D. Roviras, "PAPR reduction of post-OFDM waveforms contenders for 5G & beyond using SLM and TR algorithms," in *Proc. 25th Int. Conf. Telecommun. (ICT)*, Jun. 2018, pp. 104–109.
[14] E. Hong, H. Kim, K. Yang, and D. Har, "Pilot-aided side information detection in SLM-based OFDM systems," *IEEE Trans. Wireless Commun.*, vol. 12, no. 7, pp. 3140–3147, Jul. 2013.
[15] Y. A. Jawhar, L. Audah, M. A. Taher, K. N. Ramli, N. S. M. Shah, M. Musa, and M. S. Ahmed, "A review of partial transmit sequence for PAPR reduction in the OFDM systems," *IEEE Access*, vol. 7, pp. 18021–18041, 2019.
[16] D. Qu, L. Li, and T. Jiang, "Invertible subset LDPC code for PAPR reduction in OFDM systems with low complexity," *IEEE Trans. Wireless Commun.*, vol. 13, no. 4, pp. 2204–2213, Apr. 2014.
[17] K. Tahkoubit, A. Ali-Pacha, H. Shaiek, and D. Roviras, "Iterative dichotomy PAPR reduction method for multicarrier waveforms," *IEEE Commun. Lett.*, vol. 23, no. 11, pp. 2073–2076, Nov. 2019.
[18] T. Florent, "Power amplifier design for 5G applications in 28 nm FD-SOI technology," Ph.D. dissertation, Dept. Electron., Bordeaux Univ., Bordeaux, France, 2018.
[19] P. Garcia-Ducar, J. de Mingo, P. L. Carro, and A. Valdovinos, "Design and experimental evaluation of a LINC transmitter for OFDM systems," *IEEE Trans. Wireless Commun.*, vol. 9, no. 10, pp. 2983–2987, Oct. 2010.
[20] K. Tahkoubit, H. Shaiek, D. Roviras, and A. Ali-Pacha, "Energy efficiency comparison of outphasing and IDP techniques with non-linear power amplifiers," in *Proc. 3rd Int. Conf. Adv. Commun. Technol. Netw. (CommNet)*, Morocco, North Africa, Sep. 2020, pp. 1–5.
[21] P. Kaur, "Complementary cumulative distribution function for performance analysis of OFDM signals," *IOSR J. Electron. Commun. Eng.*, vol. 2, no. 5, pp. 5–7, 2012.
[22] M. DeGroot and M. Schervish, *Probability and Statistics*. London, U.K.: Pearson, 2014, p. 213.
[23] D. Hammou, E. Moldovan, and S. O. Tatu, "Novel MHMIC millimeter wave power divider/combiner," in *Proc. 24th Can. Conf. Electr. Comput. Eng. (CCECE)*, Niagara Falls, ON, USA, May 2011, pp. 280–283.

KHALED TAHKOUBIT (Student Member, IEEE) received the bachelor's degree in electronic engineering and the master's degree in telecommunication and networks from University Ammar Tlidji Laghouat (UATL), in 2014 and 2016, respectively. He is currently pursuing the Ph.D. degree with the Laboratory of Coding and Information Security, USTO-MB, Algeria, where his current research includes techniques for reducing the imperfections of the radio frequency chain for post-5G multi-carrier waveforms. In December 2020, he joined the Conservatoire National des Arts et Métiers as a Temporary Lecturer and a Research Assistant in electronics and signal processing. His research interests include the performance analysis of multicarrier modulation, communication systems, networks, multi-carrier waveforms, signal processing, and PAPR reduction.

HMAIED SHAIEK (Member, IEEE) received the bachelor's degree from the National Engineering School of Tunis, in 2002, the master's degree from the Université de Bretagne Occidentale, in 2003, and the Ph.D. degree from the Lab-STICC CNRS Team, Telecom Bretagne, in 2007. He was with Canon Inc., until 2009. He left the industry to integrate with the École Nationale d'Ingénieurs de Brest as a Lecturer, from 2009 to 2010. In 2011, he joined the Conservatoire National des Arts et Métiers as an Associate Professor in electronics and signal processing. He holds three patents and has authored or coauthored 15 journal articles and over 40 conference papers. His research interests include the performance analysis of multicarrier modulations with nonlinear power amplifiers, PAPR reduction, and power amplifier linearization. He contributed to the FP7 EMPHATIC European Project and is involved in two national projects, such as Accent5 and Wong5, funded by the French National Research Agency.

DANIEL ROVIRAS (Senior Member, IEEE) was born in 1958. He received the bachelor's degree from SUPÉLEC, Paris, France, in 1981, and the Ph.D. degree from the National Polytechnic Institute of Toulouse, Toulouse, France, in 1989. He spent in the industry as a Research Engineer for seven years. He joined the Electronics Laboratory, École Nationale Supérieure d'Électrotechnique, d'Électronique, d'Informatique, et des Télécommunications (ENSEEIHT), where he joined the Engineering School in 1992 as an Assistant Professor and has been a Full Professor since 1999. Since 2008, he has been a Professor with Conservatoire National des Arts et Métiers (CNAM), Paris, where his teaching activities are related to radiocommunication systems. He is currently a member of the CEDRIC Laboratory, CNAM. His research activity was first centered around transmission systems based on infrared links. Since 1992, his topics have been widened to more general communication systems, such as mobile and satellite communications systems, equalization, predistortion of nonlinear amplifiers, and multicarrier systems.

SALIM FACI (Senior Member, IEEE) received the Dipl. Ing. degree in electronics from Mouloud Mammeri University, in 2001, the M.D. degree in electronics and the Ph.D. degree in electronics, optronics, and systems from Pierre et Marie Curie University (UPMC), in 2003 and 2007, respectively. His Ph.D. research focused on photoconductive switches modeling and optical control of microwave oscillators. He is currently with the Electronic, Communication Systems and Microsystems Laboratory (ESYCOM) where his research is focused on microwave photonics, which includes radio over fiber systems, photonic generation of mm-wave signals, and optoelectronic devices modeling. His research interest includes numerical simulation methods for nanophotonic devices.

ADDA ALI-PACHA was born in Algeria, in 1960. He received the bachelor's degree in telecommunications from the Institute of Telecommunication of Oran–Algeria (ITO), in 1986, the master's degree in mathematics, in June 1986, the Magister degree in signal processing, in November 1993, and the Ph.D. degree in safety data, in 2004. He was with the Telecommunications Administration (PTT Oran–Algeria) as the Head of telephone traffic for two years (1986–1988). Since 1989, he has been with the Electronics Institute, University of Sciences and Technology of Oran (USTO), Algeria, as a Professor (Teacher/Researcher). He is currently the Head of the Coding and Information Security Research Laboratory. His research interests include digital communications and cryptography.